Wake-up Radio Integration In IoT Sensors: A SimulationBased Analysis Of Network Lifetime And Performance Tradeoffs

Junlei Dong[1,2] and Shuai Fu[3*]

[1] School of Artificial Intelligence and Information Technology, Henan Polytechnic, Zhengzhou 450046, Henan, China
[2] Henan Engineering Research Center of Fault-Tolerant Server, Zhengzhou 450046, Henan, China
[3] Changchun Humanities and Sciences College, Changchun 130117, Jilin, China
[*] Corresponding author. E-mail: fushuai@ccrw.edu.cn; fus0629@126.com

Received: December 30, 2025; Accepted: August 03, 2026

The deployment of long-term autonomous Internet of Things (IoT) sensor networks is constrained by the finite energy budget of battery-powered nodes. Although Synchronous Duty Cycling (SDC) is widely used to reduce idle-listening energy, its scalability is limited by synchronization overhead and packet collisions. This study quantitatively compares Wake-up Radio (WuR)-assisted communication with SDC and Always-On baselines using a discrete-event simulation framework. The model incorporates long-term battery depletion, stochastic packet generation, collision-induced packet loss, and channel loss over a 365-day horizon. Results from a simulated 50-node network show that, although SDC extends network lifetime to approximately 45 days, its packet loss increases superlinearly and reaches approximately 16% under high-density conditions because of contention within synchronized active windows. In contrast, the WuR-assisted approach maintains packet loss below 1.2% across load levels and retains 34.6% of battery capacity after one year, corresponding to a projected lifetime of more than 1.5 years. With an energy cost of 30.6 mJ per successful packet, WuR achieves a 13.5-fold improvement over SDC. These results indicate that WuR-assisted communication is a more suitable architecture for scalable, latency-sensitive, and ultra-long-lived IoT deployments.

Keywords: Wake-up Radio; Internet of Things; Energy Efficiency; Network Lifetime; Simulation
© The Author('s). This is an open-access article distributed under the terms of the Creative Commons Attribution License (CC BY 4.0), which permits unrestricted use, distribution, and reproduction in any medium, provided the original author and source are cited.

http://dx.doi.org/10.6180/jase.202701_36.045

1. Introduction

The rapid expansion of the IoT has led to the massive deployment of smart sensors for environmental monitoring, industrial automation, and healthcare applications [1, 2]. A fundamental challenge in these deployments is the energy-latency-reliability trade-off. Battery-powered nodes must often operate for years without maintenance [3], yet traditional radio transceivers consume significant power during idle listening, which can account for up to 99% of total energy usage in low-traffic applications [4, 5].

To mitigate idle-listening energy consumption, SDC is widely used to periodically sleep the radio. While SDC reduces energy compared to Always-On baselines [6], it introduces inherent latency and requires strict network-wide time synchronization, which consumes additional energy [7]. Critically, as network density increases, SDC forces nodes to contend for the medium during narrow active windows, leading to collision clusters and scalability bottlenecks.

WuR technology offers a hardware-based solution by employing a secondary, ultra-low-power receiver to monitor the channel continuously, allowing the main radio to sleep until triggered [8]. While WuR hardware is maturing with standards such as IEEE 802.11ba [9], existing literature often lacks rigorous comparisons of WuR against SDC under realistic network impairments and long-term battery depletion dynamics [10].

To address these gaps, this study presents a comprehensive simulation that compares the Always-On, SDC, and WuR strategies. A discrete-event framework modeling stochastic packet generation, collision-induced packet loss, and battery depletion over a 365-day horizon is employed.

This study is motivated by the practical need to design battery-powered IoT sensor networks that can operate reliably for months or years without frequent maintenance. Although SDC can reduce idle-listening energy consumption, its dependence on periodic wake-up schedules introduces latency, synchronization overhead, and collision clustering, especially under dense-network and stochastic-traffic conditions. By contrast, many existing WuR studies focus mainly on hardware characterization, short-term performance evaluation, or simplified channel assumptions. Therefore, a long-horizon, system-level simulation framework is required to jointly evaluate battery depletion, packet collisions, channel loss, latency, and energy efficiency. Accordingly, this study compares Always-On, SDC, and WuR-assisted communication strategies through a 365-day discrete-event simulation to clarify their long-term suitability for scalable and sustainable IoT deployments.

The key contributions of this study are:

- Quantification of long-term sustainability: The study demonstrates that WuR enables multi-year operation, whereas SDC fails within months because of synchronization and idle-listening overhead.
- Analysis of scalability and reliability: The study identifies a superlinear increase in SDC packet loss at high node densities due to collision clustering, in contrast to the stable reliability of asynchronous WuR communication.
- Validation of energy-latency decoupling: The study shows that WuR can provide the near-zero-latency performance of Always-On operation while maintaining energy efficiency superior to aggressive duty cycling.

2. Related studies

The minimization of energy consumption in battery-constrained IoT networks remains a critical research focus, particularly for applications requiring multi-year operational lifetimes. Traditional approaches have relied heavily on SDC and sleep scheduling to mitigate the high cost of idle listening. Park et al. [4] proposed mechanisms such as down-clocking to reduce energy during idle states in Wi-Fi, while Liu et al. [11] introduced concurrent low-power listening paradigms to optimize duty-cycling communication. Comprehensive reviews of medium access control (MAC) protocols, such as those by Amin et al. [6], highlight that while SDC significantly reduces energy compared to always-on baselines, it inherently introduces latency and synchronization overhead. Furthermore, the approach proposed by Kuaban et al. [3], which models battery-depletion attacks, emphasizes that energy-constrained nodes remain vulnerable to exhaustion if sleep schedules are not strictly maintained. However, as network density increases, synchronized approaches often struggle to scale while avoiding packet collisions, creating bottlenecks in dense IoT deployments.

To address the limitations of SDC, WuR technology has emerged as a hardware-based solution to eliminate idle listening. Recent surveys by Chen et al. [8] and Spohn et al. [12] provide comprehensive analyses of WuR architectures, highlighting that while passive and semi-passive front-ends can achieve nanowatt-level power consumption, they face significant trade-offs regarding sensitivity and noise resilience. The maturation of this technology is evidenced by recent standardization efforts; Wang et al. [13] review the integration of wake-up signals into 4G/5G cellular IoT, while Sanchez-Vital et al. [9] demonstrate that the IEEE 802.11ba amendment can extend battery life by 500% in Wi-Fi mesh networks. On the hardware implementation side, Schulthess et al. [14] characterized WakeMod, an open-source module that consumes only 6.9 μW, demonstrating the feasibility of discrete WuR integration. Despite these hardware advancements, these studies primarily focus on device-level characterization or single-hop links, often neglecting the system-level complexities of multi-hop interference and routing.

Recent research has attempted to integrate WuR into higher-layer network protocols. Shah et al. [10] proposed DU-TSCH, a dual-mode MAC that separates low-delay and best-effort traffic to improve reliability, while Ding and Tatinian [15] developed a hierarchical simulation framework to model realistic hardware behaviors, such as false wake-ups. In specific application domains, Panga and Borkotoky [16] and Shah et al. [17] utilized WuR for UAV-assisted data collection, employing clustering techniques to optimize energy efficiency. Similarly, Mosavat et al. [18] explored WuR for batteryless, energy-harvesting nodes, demonstrating significant goodput improvements. However, these solutions often rely on centralized scheduling or specific topologies that do not generalize to autonomous, distributed sensor networks. Furthermore, alternative long-range approaches such as the preamble-sampling methods for LoRa proposed by Leenders et al. [19] and Hong et al. [20] show that while duty-cycling can be optimized, it still incurs high airtime costs compared to dedicated WuR

hardware.

A persistent gap in the literature is the lack of rigorous, long-term comparative analyses that account for network impairments. Deshpande et al. [21] noted that wake-up messages are susceptible to channel erasure and interference, yet few studies quantify the impact of these collisions over long durations. While Rup and Bajic [22] frame WuR as a key enabler for Green IoT, and older works such as Ghribi and Meddeb [23] began exploring collision avoidance, there is a scarcity of studies that simulate the energy-latency-reliability trade-off under stochastic traffic for extended periods. Most existing comparisons, such as those in [15] or [24], rely on short-term metrics or idealized channel models. This study addresses these deficiencies by providing a side-by-side evaluation of SDC and WuR strategies, specifically modeling the impact of collisions and battery depletion in a realistic, long-term simulation environment.

3. Materials and methods

3.1. Simulation Framework and Software Environment

To ensure a rigorous, reproducible, and unbiased comparison of power-management strategies in battery-constrained IoT networks, a discrete-event simulation framework in Python 3.10 was developed. The simulation environment was built from first principles to avoid introducing implicit assumptions from existing network simulators. Core functionality was implemented using SimPy 4.0.1 for discrete-event modeling, NumPy 1.24 for stochastic process generation and numerical computation, Pandas 2.0 for structured data aggregation and analysis, and Matplotlib 3.7 with Seaborn 0.12 for statistical visualization.

All simulations were executed under reproducible random states to enable exact replication of results. To quantify statistical robustness, each experimental configuration was run across five independent random seeds, with aggregated results reported as mean $\pm$ standard deviation. This multi-seed protocol accounts for the stochastic nature of Poisson packet generation and ensures that observed performance differences reflect system behavior rather than sampling artifacts (Table 1).

3.2. Network Topology and Traffic Model

The simulated network consisted of N homogeneous sensor nodes operating in a single-hop star topology, communicating with a central gateway. For the baseline configuration, $N = 50$ nodes were deployed, with sensitivity analyses conducted at $N \in \{20, 100\}$ to assess scalability. All nodes were assumed to be within communication

Table 1. Main simulation parameters and assumptions

Category	Parameter	Setting	Purpose
Simulation environment	Software	Python 3.10, SimPy 4.0.1, NumPy 1.24, Pandas 2.0, Matplotlib 3.7	Reproducible discrete-event simulation
Randomization	Number of seeds	5 independent seeds	Statistical robustness
Network topology	Topology	Single-hop star topology	Isolation of energy-management effects
Network size	Baseline nodes	50 nodes	Main comparative scenario
Network size	Sensitivity nodes	20 and 100 nodes	Scalability analysis
Traffic model	Packet-generation process	Poisson process	Stochastic IoT traffic modeling
Traffic rate	Mean inter-packet interval	600 s baseline; 300 s and 1200 s sensitivity	Traffic-load analysis
Packet size	Data payload	1024 bits	Fixed packet length
Data rate	Transmission rate	250 kbps	Packet airtime calculation
Battery model	Battery type	CR2032 coin cell, 3.0 V, 225 mAh	Initial energy budget
Radio power	TX power	57 mW	Transmission energy
Radio power	RX/listening power	62.4 mW	Idle-listening energy
Radio power	Sleep power	0.003 mW	Deep-sleep energy
Wake-up radio	WuR listening power	50 μW	Secondary receiver energy
Channel model	Channel-loss probability	1%	Non-ideal transmission modeling
Collision model	Collision condition	Overlapping packet transmissions	Shared-channel contention modeling
Baseline horizon	Short-term simulation	7 days	Baseline comparison
Long-term horizon	Sustainability simulation	365 days	Battery-lifetime evaluation

range of the gateway, abstracting away propagation and multi-hop routing complexities to isolate the fundamental energy-management trade-offs of interest.

Each node generated data packets independently according to a Poisson process with rate parameter $\lambda = \frac{1}{T_{\text{gen}}}$ and $\Delta t \sim \text{Exp}(\lambda)$, where T_{gen} represents the mean inter-packet interval. For the baseline configuration, $T_{\text{gen}} = 600$ seconds (10 minutes), reflecting typical low-rate environmental monitoring applications. Sensitivity analyses explored $T_{\text{gen}} \in \{300, 600, 1200\}$ seconds to examine behavior under varying traffic intensities. Packets were fixed at 1024 bits and transmitted at 250 kbps, yielding a nominal air time of $T_{\text{tx}} = 4.096$ milliseconds per packet.

This stochastic traffic model captures the asynchronous, event-driven nature of real-world IoT deployments where sensor readings are triggered by environmental phenomena or periodic sampling that does not align across nodes.

3.3. Energy Model and Battery Dynamics

Each sensor node was equipped with a virtual battery modeled after a CR2032 coin cell: 3.0 V nominal voltage, 225 mAh capacity, yielding an initial energy budget of:

$$E_0 = V_{\text{nom}} \times C_{\text{bat}} \times 3600 \tag{1}$$

$$E_0 = V \times C \times \frac{3600}{1000} = 3.0 \times 225 \times \frac{3600}{1000} = 2430 \text{ J} \tag{2}$$

$$E_i(t) = E_0 - \Sigma_s P_s T_{i,s}(t) \tag{3}$$

where P_s is the power consumption of state s, and $T_{i,s}(t)$ is the cumulative time spent by node i in that state up to time t. The considered states were transmission, reception/listening, deep sleep, and WuR listening. A node was considered non-operational when $E_i(t) \leq 0$. As shown in Eq. (3), power consumption profiles were derived from datasheets of representative low-power wireless transceivers (such as Texas Instruments CC2420, Nordic nRF52 series) and wake-up radio prototypes reported in recent literature. The main transceiver power states were: Transmit (TX) at $P_{\text{TX}} = 57.0$ mW, Receive/Listen (RX) at $P_{\text{RX}} = 62.4$ mW, and Sleep at $P_{\text{sleep}} = 0.003$ mW (deep sleep, $\approx$1 μA current draw). For the WuR-assisted scenario, a secondary ultra-low-power receiver was active continuously with $P_{\text{WuR}} = 0.050$ mW (50 μW, representative of state-of-the-art WuR designs).

Energy consumption was computed by integrating power over time for each operational state. For a node spending time t_{TX}, t_{RX}, t_{sleep}, and t_{WuR} in respective states, the total energy consumed is given by Eq. (4):

$$E_{\text{cons}} = P_{\text{TX}} t_{\text{TX}} + P_{\text{RX}} t_{\text{RX}} + P_{\text{sleep}} t_{\text{sleep}} + P_{\text{WuR}} t_{\text{WuR}} \tag{4}$$

A node was declared non-operational when $E(t) = E_0 - E_{\text{cons}}(t) \leq 0$. This deterministic energy model assumes ideal battery behavior (no capacity fade, constant voltage) to isolate the impact of radio power management from electrochemical effects.

3.4. Communication Scenarios and Operational Logic

Three distinct power-management strategies, each representing a fundamental class of approaches used in practice, were evaluated.

3.4.1. *Scenario A: Always-On Baseline*

In the Always-On configuration, the main radio transceiver remains continuously in the receive (RX) state, ensuring immediate packet reception capability. This represents the simplest but most energy-intensive approach, with idle listening power dominating the energy budget. Upon packet generation, the node transitions to TX for $T_{\text{tx}} = \frac{1024}{250000} = 0.004096$ s, then immediately returns to RX. No sleep state is ever entered. This scenario serves as an upper bound on responsiveness (zero latency) and a lower bound on energy efficiency.

3.4.2. *Scenario B: SDC*

The SDC protocol implements periodic sleep-wake cycles to reduce idle listening energy. Nodes operate on a fixed duty cycle period $T_{\text{dc}} = 1.0$ s, remaining in deep sleep for $T_{\text{sleep}} = 0.99$ s and waking to listen for $T_{\text{listen}} = 0.01$ s (1% duty cycle). Packet transmissions are deferred until the next active listening window, introducing latency proportional to T_{dc}.

To account for the cost of maintaining network-wide synchronization, periodic synchronization events was modeled every $T_{\text{sync}} = 3600$ s (1 hour). Each synchronization event involves a brief RX phase of $T_{\text{sync, RX}} = 0.01$ s to receive a beacon, followed by a TX phase of $T_{\text{sync, TX}} = 0.005$ s to acknowledge, consuming Eq. (5):

$$E_{\text{sync}} = P_{\text{RX}}\, T_{\text{sync, RX}} + P_{\text{TX}}\, T_{\text{sync, TX}} \tag{5}$$

This overhead, typically neglected in prior work, accounts for the practical cost of time synchronization protocols (such as TSCH, FTSP) and ensures completeness of the SDC energy model.

3.4.3. *Scenario C: WuR Assisted*

The WuR-assisted system employs a heterogeneous dual-radio architecture. The main transceiver remains in deep sleep by default, while a secondary ultra-low-power WuR continuously monitors for wake-up signals at P_{WuR}. Upon packet generation, the main radio is powered on only for the duration of transmission T_{tx}, then immediately returns to sleep. This approach eliminates idle listening of the main radio, replacing it with the microwatt-level power draw

of the WuR. Latency is effectively zero, as transmission occurs immediately upon generation without waiting for scheduled windows.

3.5. Channel Model and Packet Success Criteria

To account for network impairments, the baseline simulation was extended with an explicit channel model that captures two primary failure modes. The collision model marks packets transmitted with overlapping time intervals (i.e., $t_{\text{start},i} < t_{\text{end},j}$ and $t_{\text{start},j} < t_{\text{end},i}$ for packets i and j) as collisions, with all packets involved in a collision deemed lost. This models contention on a shared single-channel medium without CSMA/CA or other collision avoidance mechanisms. The channel loss model subjects packets that successfully avoided collisions to an independent Bernoulli trial with failure probability $p_{\text{loss}} = 0.01$ (1%), representing aggregate effects of fading, interference, and thermal noise. This probability is consistent with typical packet error rates in indoor IoT environments at moderate SNR.

A packet was classified as successfully delivered only if it avoided both collision and channel loss. Performance metrics (throughput, energy per successful packet) were computed using only successfully delivered packets, providing a realistic lower bound on network performance. Failed packets still incurred energy cost (transmission occurred but was lost), accurately reflecting wasted energy in lossy environments. This dual-failure model allows us to quantify the interaction between MAC-layer contention (higher under bursty Poisson traffic) and physical-layer reliability. Accordingly, the delivery status of each packet was determined through a two-step decision rule. First, the simulator checked whether the packet transmission interval overlapped with any other packet transmission interval on the shared channel. If an overlap occurred, all involved packets were marked as collision losses. Second, packets that avoided collision were subjected to an independent Bernoulli trial with a channel-loss probability of 1%. A packet was counted as successfully delivered only when it passed both the collision test and the channel-loss test.

3.6. Performance Metrics and Data Collection

For each node in each simulation run, detailed operational logs at packet-level granularity were recorded, including generation time, transmission start/end times, and success status. From these logs, the following metrics were computed: Node Lifetime (L_{node}), defined as total operational time in hours until battery depletion, capped at simulation duration for surviving nodes; Packets Attempted (N_{att}), representing the total number of packets generated and transmitted by a node; Packets Successful (N_{succ}), defined as the subset of attempted packets successfully delivered (no collision, no channel loss); Packet Loss Rate, calculated as $\text{PLR} = 1 - \frac{N_{\text{succ}}}{N_{\text{att}}}$; Average Latency ($\bar{l}$), measured as the mean time from packet generation to transmission start in seconds (for Always-On and WuR, latency is near-zero with immediate transmission, while for SDC, latency is due to waiting for the next listening window); Energy per Successful Packet, quantified as $E_{\text{succ}} = \frac{E_{\text{cons}}}{N_{\text{succ}}}$ in millijoules, measuring the energetic cost of useful data delivery; and Final Battery Level, expressed as a percentage of initial capacity remaining at simulation end, computed as $100 \times \frac{E_{\text{final}}}{E_0} = 100 \times \frac{E_0 - E_{\text{cons}}}{E_0}$.

Scenario-level statistics were computed by aggregating across all nodes and all seeds, reporting mean and standard deviation for each metric. This provides both central tendency (expected performance) and dispersion (robustness/variability). The packet loss rate was calculated as:

$$\text{PLR} = \frac{N_{\text{attempted}} - N_{\text{successful}}}{N_{\text{attempted}}} \tag{6}$$

where $N_{\text{attempted}}$ is the total number of generated and transmitted packets, and $N_{\text{successful}}$ is the number of packets successfully delivered. The average packet latency was calculated as:

$$L_{\text{avg}} = \frac{1}{N_{\text{successful}}} \sum (t_{\text{tx,start}} - t_{\text{gen}}) \tag{7}$$

where t_{gen} is the packet-generation time and $t_{\text{tx,start}}$ is the transmission start time. The energy cost per successful packet was calculated as:

$$E_{\text{pkt}} = \frac{E_0 - E_{\text{final}}}{N_{\text{successful}}} \tag{8}$$

where E_{final} is the remaining battery energy at the end of the simulation or at the time of node failure. This metric normalizes the total energy consumption by the amount of useful data successfully delivered.

3.7. Experimental Configurations

To ensure robustness, simulations were conducted across multiple configurations. In addition to the baseline setup defined in Sections 3.1 and 3.2 (50 nodes, 600 s interval, 7-day duration), sensitivity analyses to test scalability and traffic load were performed. These included: Low Density (20 nodes), High Density (100 nodes), and High Traffic (300 s interval). Finally, a Long-Horizon configuration extended the simulation to 365 days for the Duty-Cycled and WuR-Assisted scenarios to assess multi-year viability (Always-On was excluded due to rapid failure). All configurations used random seed replicates to ensure statistical validity.

Table 2. Discrete-event simulation procedure

Algorithm 1. Discrete-event simulation procedure.
Step 1: Initialize the simulation environment, random seed, network size, battery capacity, radio power states, traffic rate, and simulation horizon. Step 2: For each node, generate packet-arrival events according to the Poisson traffic model. Step 3: For each packet event, determine the active communication scenario: Always-On, SDC, or WuR-assisted operation. Step 4: Update the node radio state according to the selected scenario and compute the corresponding energy consumption. Step 5: For SDC, defer packet transmission until the next active listening window and include periodic synchronization overhead. Step 6: For WuR-assisted communication, keep the main radio in sleep mode and activate it only during packet transmission. Step 7: Apply the channel model by checking collision overlap and stochastic channel loss. Step 8: Record packet status, latency, energy consumption, and remaining battery level. Step 9: Repeat the simulation for all nodes, configurations, and random seeds. Step 10: Aggregate the results and compute mean and standard deviation for lifetime, packet loss rate, latency, energy per successful packet, throughput, and final battery level.

3.8. Data Processing and Statistical Analysis

Raw simulation outputs (node-level logs, packet-level events) were exported to CSV format for reproducibility and post-processing. All analyses were performed using Pandas and NumPy, with visualizations generated using Matplotlib and Seaborn. Statistical summaries report means $\pm$ standard deviation across seeds, with individual node distributions visualized using box plots to reveal both central tendency and tail behavior.

Energy consumption breakdowns were computed by multiplying time spent in each state by the corresponding power level, aggregating across all nodes per scenario. This state-level accounting provides mechanistic insight into the sources of energy drain. For long-term simulations, survival curves (fraction of nodes remaining operational vs. time) and projected multi-year battery lifetime by extrapolating observed depletion rates were computed.

3.9. Methodological Assumptions and Scope

Several assumptions were adopted to keep the simulation focused on the energy-management behavior of the compared communication strategies. First, a single-hop star topology was used to isolate the effects of radio duty cycling, wake-up operation, packet collisions, and battery depletion without introducing additional routing overhead. Second, homogeneous sensor nodes were assumed so that performance differences could be attributed to the communication strategy rather than hardware heterogeneity. Third, the battery model assumed constant nominal voltage and did not include temperature-dependent capacity variation or electrochemical aging. Fourth, the channel model considered packet collisions and independent stochastic channel loss but did not include capture effects, retransmission protocols, adaptive modulation, or multi-channel access. These assumptions define the scope of the present study and provide a controlled basis for comparing Always-On, SDC, and WuR-assisted communication. Future extensions can incorporate multi-hop routing, heterogeneous hardware, adaptive medium-access control, and experimental testbed validation.

4. Results and discussion

4.1. Baseline Network Performance: 7-Day, 50-Node Configuration

The key performance indicators for the baseline configuration are summarized in Table 3. The Always-On scenario failed on average after 10.8 hours, confirming that continuous idle listening is unsustainable for battery-powered nodes. In contrast, both Duty-Cycled and WuR-Assisted nodes survived the full 7-day simulation. However, efficiency differences were stark: WuR nodes consumed 92% less energy than SDC nodes, while maintaining 98.75% battery capacity, compared with SDC's 84.38%. Furthermore, WuR achieved a packet loss rate of only 1.1%, compared with 8.7% for SDC, demonstrating superior reliability even under standard load conditions.

Table 3. Summary of Key Performance Indicators (Baseline Configuration)

Metric	Always-On	Duty-Cycled	WuR-Assisted
Avg. Lifetime (Days)	0.45 ± 0.00	7.00 ± 0.00	7.00 ± 0.00
Total Packets Successful (Network)	16,003	229,850	249,058
Avg. Final Battery (%)	0.00 ± 0.00	84.38 ± 0.00	98.75 ± 0.00
Energy per Successful Packet (mJ)	38,560 ± 4,953	413.3 ± 13.4	30.6 ± 1.0
Packet Loss Rate	0.0099 ± 0.012	0.0876 ± 0.0088	0.0111 ± 0.0031
Avg. Latency (ms)	0.0 ± 0.0	509.9 ± 9.1	0.0 ± 0.0

4.1.1. Network Lifetime and Battery Depletion

While the Always-On baseline proved non-viable, the survival curves of the remaining strategies diverged significantly. Duty-Cycled nodes consumed approximately 380 J over the week, a linear drain driven by the fixed costs of synchronization and the 1% duty cycle. WuR-Assisted nodes, however, operated near-losslessly, consuming only ∼30 J. Fig. 1 (left) illustrates the final battery distribution, showing tight clustering near 100% for WuR, whereas SDC exhibits broader variance due to the stochastic nature of packet waiting times. Fig. 1 (right) confirms that throughput was nearly identical across viable strategies (∼920-990 packets), meaning the 13-fold energy reduction achieved by WuR comes without compromising data delivery. This demonstrates that eliminating the main radio's idle listening is far more effective than merely duty-cycling it.

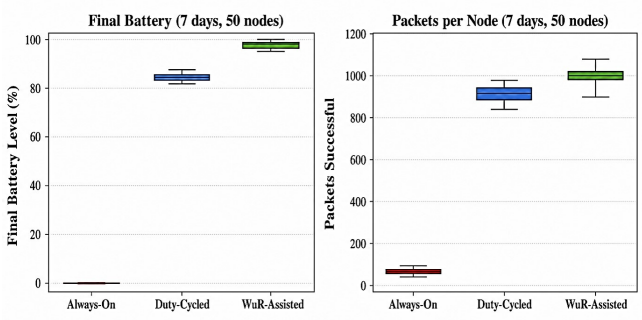


Fig. 1. Baseline network lifetime and throughput distributions

4.1.2. Network Throughput and Packet Delivery

Despite the Always-On scenario's energy failure, it transmitted 16,003 packets network-wide before collapse, averaging ∼64 packets per node. However, this represents less than 7% of the throughput achieved by the two viable strategies. Duty-Cycled and WuR-Assisted scenarios delivered 229,850 and 249,058 successful packets, respectively, over the 7 days, corresponding to approximately 920–996 packets per node. The slightly higher throughput for WuR (+8.3% vs. Duty-Cycled) is attributable to lower packet loss rather than higher generation rates. Both scenarios generated similar numbers of packets (stochastic Poisson process identical across scenarios), but WuR experienced significantly lower loss.

4.1.3. Energy Efficiency: Cost per Successful Packet

Energy per successfully delivered packet provides a normalized efficiency metric that accounts for both total energy consumption and useful work accomplished. Always-On incurred an extraordinary cost of 38,560 ± 4,953 mJ per successful packet, reflecting massive wasted energy during idle listening relative to the brief transmission duration. High variance (±13%) arises from node-to-node differences in the timing of battery depletion relative to packet generation events. Duty-Cycled operation reduced this cost by nearly two orders of magnitude to 413.3 ± 13.4 mJ per packet, confirming the well-established benefit of duty cycling. However, WuR-Assisted achieved a further order-of-magnitude improvement to 30.6 ± 1.0 mJ per packet, representing a 13.5× efficiency gain over SDC and a 1,260× gain over Always-On. Low variance (±3%) across seeds demonstrates the robustness of this advantage.

Fig. 2 presents a multi-panel visualization of the trade-offs among energy efficiency, packet loss, and latency. The logarithmic scale on the energy axis clearly illustrates the orders-of-magnitude differences. These results quantitatively validate the theoretical expectation that replacing high-power idle listening with microwatt-level WuR monitoring fundamentally alters the system's energy profile.

4.1.4. Reliability: Packet Loss Rates Under Network Impairments

The inclusion of collisions and channel loss revealed meaningful differences in reliability across scenarios. Always-On and WuR exhibited similar low loss rates (∼1.0–1.1%), consistent with the 1% channel-loss model and minimal collision probability at low node density during the brief operational window of Always-On nodes. In contrast, Duty-Cycled nodes experienced 8.76 ± 0.88% packet loss, an 8-fold increase compared to WuR. This elevated loss arises from temporal clustering: since all nodes synchronize their transmissions to narrow 10 ms listening windows, Poisson-

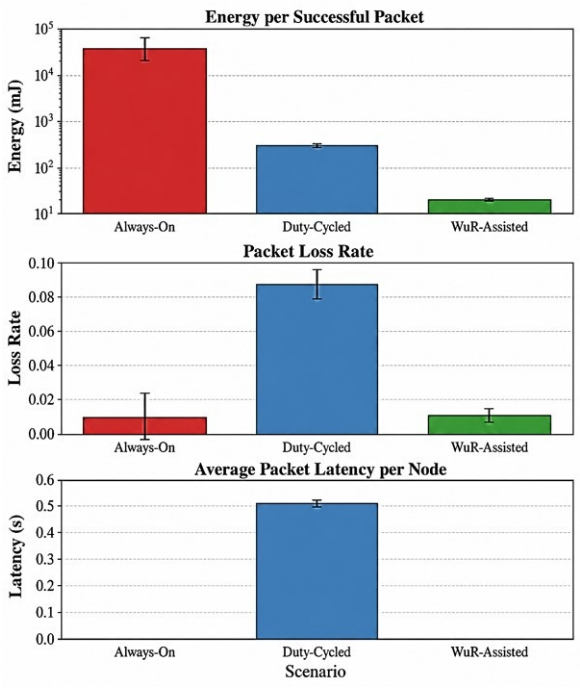


Fig. 2. Performance trade-offs across communication strategies

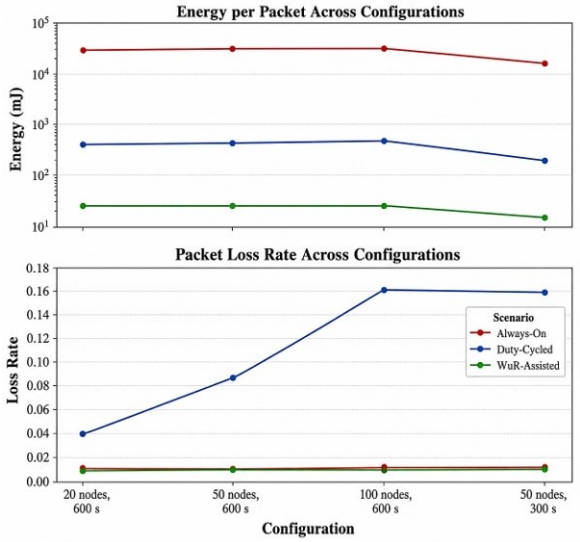


Fig. 3. Sensitivity of energy efficiency and reliability to network configuration

generated packets from multiple nodes frequently collide within these windows. The collision rate scales with node density and traffic intensity, a vulnerability inherent to synchronous MAC protocols. WuR's near-zero latency and asynchronous transmission eliminate temporal clustering, distributing transmissions uniformly over time and drastically reducing collision probability. This represents a previously under-appreciated advantage of the WuR paradigm: superior reliability in addition to superior energy efficiency.

4.1.5. Latency Analysis

Average packet latency for Always-On and WuR scenarios was effectively zero (within simulation time resolution), as packets are transmitted immediately upon generation. For Duty-Cycled nodes, mean latency was 509.9 ± 9.1 milliseconds, closely matching the theoretical expectation of 500 ms for uniformly distributed packet arrivals within a 1-second cycle. Low variance confirms consistent behavior across seeds. This $\sim$0.5-second delay is acceptable for many low-rate IoT applications but problematic for latency-sensitive use cases such as event-driven alarms or closed-loop control. WuR provides the latency profile of Always-On with energy efficiency far surpassing Duty-Cycled, effectively decoupling the traditional energy-latency trade-off.

4.2. Sensitivity Analysis: Robustness to Network Configuration

To assess the generalizability of baseline findings, node density and traffic intensity across four configurations were varied. Table 4 summarizes energy per successful packet and packet loss rate for each configuration and scenario. All configurations ran for 7 days with 5 seeds per scenario.

4.2.1. Impact of Node Density

Increasing node count from 20 to 100 while holding traffic rate constant (600 s interval) revealed divergent trends. WuR energy efficiency remained remarkably stable ($\sim$30.6 mJ/packet across all densities), as transmission timing is independent of other nodes. WuR loss rate also remained low and constant ($\sim$1.1%), constrained primarily by the 1% channel-loss model.

In contrast, Duty-Cycled energy per packet increased from 392.8 to 449.7 mJ (+14.5%) with density, reflecting higher collision rates that waste energy on unsuccessful transmissions. More strikingly, the Duty-Cycled loss rate increased dramatically from 3.98% (20 nodes) to 16.10% (100 nodes), a 4-fold increase. This super-linear growth confirms that collision probability scales nonlinearly with the number of nodes contending within synchronized windows, a fundamental scalability limitation of SDC. Always-On energy per packet remained roughly constant across densities ($\sim$38 kJ/packet), as idle listening dominates energy consumption regardless of contention. Its loss rate stayed near the channel loss floor ($\sim$1%), but this seemingly high reliability is meaningless given the scenario's non-viability due to energy exhaustion. Fig. 3 depicts trends in energy efficiency and loss rate across configurations. The diverging trajectories of Duty-Cycled (degrading) vs. WuR (stable) as

Table 4. Sensitivity of Energy Efficiency and Reliability to Network Load

Configuration	Scenario	Energy/Packet (mJ)	Packet Loss Rate
Low Density (20 nodes)	Always-On	38,148 ± 4,959	0.0106 ± 0.012
	Duty-Cycled	392.8 ± 12.2	0.0398 ± 0.0066
	WuR-Assisted	30.6 ± 0.9	0.0099 ± 0.0032
Baseline (50 nodes)	Always-On	38,577 ± 4,931	0.0104 ± 0.012
	Duty-Cycled	413.2 ± 13.4	0.0876 ± 0.0088
	WuR-Assisted	30.6 ± 1.0	0.0109 ± 0.0031
High Density (100 nodes)	Always-On	38,406 ± 4,802	0.0115 ± 0.013
	Duty-Cycled	449.7 ± 14.5	0.1610 ± 0.011
	WuR-Assisted	30.6 ± 1.0	0.0110 ± 0.0033
High Traffic (300 s)	Always-On	19,099 ± 1,760	0.0115 ± 0.0089
	Duty-Cycled	224.4 ± 5.2	0.1586 ± 0.0082
	WuR-Assisted	15.4 ± 0.4	0.0113 ± 0.0025

density increases underscore WuR's superior scalability.

4.2.2. Impact of Traffic Intensity

Doubling the traffic rate (halving the inter-packet interval from 600 to 300 seconds) increased the offered load while maintaining the node count at 50. Interestingly, energy per successful packet decreased for all scenarios (Always-On: 19,099 mJ; Duty-Cycled: 224.4 mJ; WuR: 15.4 mJ), because fixed idle/sleep power is now amortized over more useful transmissions. This economy of scale effect is most pronounced for WuR, which decreases from 30.6 to 15.4 mJ (-50%), indicating that WuR efficiency improves with higher utilization. However, the duty-cycled loss rate remained elevated at 15.86%, only marginally lower than the high-density case, despite fewer nodes, because a doubled traffic rate increases collision probability within each listening window. WuR loss remained low ($\sim$1.13%), indicating that even under doubled load, asynchronous transmission avoids contention effectively. These trends suggest that WuR's advantages strengthen rather than diminish under realistic IoT deployment conditions (moderate-to-high node counts, variable traffic patterns).

4.3. Long-Term Network Sustainability: 365-Day Simulation

The simulation was extended to 365 days for the Duty-Cycled and WuR-Assisted scenarios, while the Always-On scenario was excluded because it fails within hours to provide insights into multi-month and multi-year behavior. Table 5 presents long-term performance metrics.

4.3.1. Duty-Cycled Long-Term Limitations

Duty-Cycled nodes survived an average of 44.8 days ($\sim$6.4 weeks) before battery exhaustion, well short of the desired multi-year operational lifetime for autonomous IoT deployments. Linear extrapolation of the 7-day energy consumption rate (84.4% remaining after 7 days $\rightarrow$ $\sim$15.6% consumed) predicts depletion around day 45, closely matching observed results. This consistency confirms that the energy model scales linearly over time under constant traffic conditions. Despite lasting only 12.3% of the simulation period, Duty-Cycled nodes delivered 882,469 successful packets network-wide, demonstrating that substantial data can be collected before failure. However, the network becomes nonfunctional after 45 days, necessitating either costly battery replacement or energy-harvesting infrastructure.

4.3.2. WuR Long-Term Viability

In stark contrast, all WuR-Assisted nodes survived the full 365-day simulation, retaining 34.61 ± 0.002% of initial battery capacity. Remarkably low variance ($\pm$0.0006% relative) across seeds indicates highly predictable long-term behavior. At this depletion rate, nodes would last approximately 1.5 years before exhaustion (extrapolating linearly: 365 days consumed 65.4% $\rightarrow$ 100% consumed at $\sim$558 days). WuR nodes delivered 7.80 million successful packets over the year, an 8.8$\times$ improvement over Duty-Cycled throughput solely due to extended operational lifetime (packets per day were similar across viable scenarios). Energy per successful packet remained consistent at 30.6 mJ across 7-day and 365-day horizons, confirming the scalability of efficiency over time. Fig. 4 presents comparisons of long-term lifetime and final battery performance. The dramatic disparity (45 days vs. 365 days, 0% vs. 35% remaining) illustrates that WuR is not merely incrementally better, but categorically different in enabling truly long-term autonomous operation.

4.4. Energy Consumption Breakdown by Operational State

To elucidate the mechanistic origins of observed energy differences, total energy consumption by node state (Transmit, Receive, Sleep, WuR Listen) was decomposed. Table 6

Table 5. Long-Term Network Sustainability (365-Day Simulation, 50 Nodes)

Metric	Duty-Cycled	WuR-Assisted
Avg. Lifetime (Days)	44.8 ± 0.0	365.0 ± 0.0
Final Battery (%)	0.00 ± 0.00	34.61 ± 0.002
Total Packets Successful (Network)	882,469	7,797,497
Energy per Successful Packet (mJ)	413.1 ± 5.4	30.6 ± 0.1
Packet Loss Rate	0.0872 ± 0.0034	0.0107 ± 0.0004

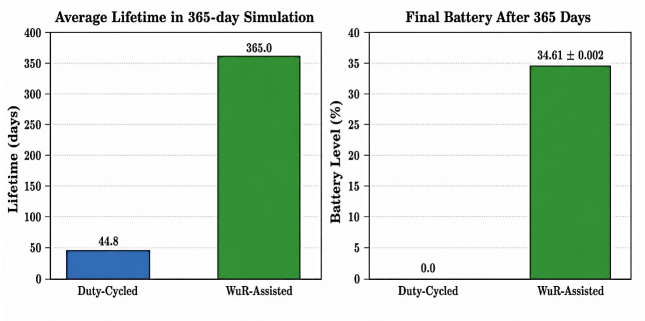


Fig. 4. Long-term network sustainability (365-day simulation, 50 nodes, 3 seeds)

presents state-level energy accounting for the 7-day baseline configuration.

4.4.1. Energy Inefficiency of Always-On Operation

Always-On energy is 99.99% idle listening (RX), with negligible transmission cost (<0.01%). This extreme imbalance confirms that idle listening is the dominant energy drain, consuming ∼2430 J to deliver ∼64 packets, an energetic cost of 38 J per packet. Given that actual packet transmission consumes only ∼0.23 mJ (57 mW × 4.096 ms), the efficiency loss is 160,000×. This quantifies the fundamental unsustainability of continuous idle listening.

4.4.2. Duty-Cycled Energy Distribution

Duty-cycling reduces RX energy by 85% (369.8 J vs. 2429.5 J) through periodic sleep, but RX still constitutes 97.5% of total consumption. Sleep energy (4.46 J) and TX energy (5.15 J) are negligible relative to the others. The persistence of RX dominance reflects the 1% duty cycle: even at 10 ms per second, RX power (62.4 mW) is 20,800× higher than sleep power (0.003 mW), so brief listening periods accumulate substantial energy. Synchronization overhead contributes an estimated 3–5 J over 7 days (168 sync events × ∼0.02 J each), a minor but non-negligible cost that justifies explicit modeling.

4.4.3. WuR Energy Transformation

WuR fundamentally restructures the energy profile: RX energy is eliminated entirely, replaced by WuR Listen energy (25.33 J, 83% of total). TX energy (5.11 J, 17%) becomes non-negligible, as the energy budget is now dominated by productive work rather than idle overhead. The WuR energy (25.33 J) is 14.6× lower than Duty-Cycled RX energy (369.8 J), despite being always on, because the WuR power draw is three orders of magnitude lower than the main radio's RX power. This breakdown provides a mechanistic explanation for WuR's efficiency: by substituting a 50 μW secondary receiver for a 62.4 mW primary receiver during idle periods, the system achieves a three orders-of-magnitude reduction in idle power, which directly translates into the observed order-of-magnitude reduction in total energy.

4.5. Overall Discussion and Implications

The results provide a quantitative foundation for evaluating power-management strategies in battery-constrained IoT deployments. The Always-On approach, while conceptually simple, is categorically unsuitable for autonomous operation, exhibiting sub-day lifetimes and energy costs that are three orders of magnitude higher than those of viable alternatives. This finding, consistent with decades of research on wireless sensor networks, underscores the fundamental necessity of power management. Synchronous Duty Cycling emerges as a viable medium-term solution, extending network lifetime to weeks or months with moderate energy efficiency (413 mJ/packet). However, SDC suffers from two critical limitations revealed by sensitivity and long-term analyses. First, packet loss rates escalate from ∼4% (low density) to 16% (high density/traffic) due to collision clustering within synchronized windows, fundamentally limiting scalability. Second, depletion within 45 days falls short of the multi-year operational lifetimes required for economically viable autonomous sensing.

Wake-up Radio technology addresses both limitations, achieving order-of-magnitude energy efficiency (30.6 mJ/packet, a 13.5× improvement over SDC), scalable reliability (loss rates bounded near 1%), and zero-latency operation. These combined advantages position WuR as a Pareto-optimal solution in the energy-latency-reliability trade-off space, dominating both Always-On (lower en-

Table 6. Average Energy Consumption Breakdown per Node (7-Day Baseline)

Scenario	TX Energy (J)	RX Energy (J)	Sleep Energy (J)	WuR Listen Energy (J)	Total (J)
Always-On	0.21 ± 0.03	2429.5 ± 0.0	0.0 ± 0.0	0.0 ± 0.0	2429.7 ± 0.0
Duty-Cycled	5.15 ± 0.16	369.8 ± 11.3	4.46 ± 0.14	0.0 ± 0.0	379.4 ± 11.6
WuR-Assisted	5.11 ± 0.16	0.0 ± 0.0	0.0 ± 0.0	25.33 ± 0.79	30.44 ± 0.95

ergy, equal latency) and Duty-Cycled (lower energy, lower latency, higher reliability).

While the results strongly favor WuR, practical deployment requires consideration of trade-offs not captured in this energy-centric analysis. Hardware cost and complexity increase with the addition of a secondary receiver, although integration into commercial SoCs is mitigating this barrier. The range limitations of lower-sensitivity WuR receivers may necessitate hybrid approaches in multi-hop networks. Furthermore, while SDC incurs synchronization overhead that scales with network size, WuR eliminates this requirement, thereby providing robustness to node mobility and intermittent connectivity. The findings align with and extend prior WuR evaluations by providing quantitative validation of theoretical advantages over realistic timescales and demonstrating robustness to network conditions. The 365-day simulation specifically addresses a gap in the literature by validating WuR as a pathway to multi-year autonomous operation.

This study makes several simplifying assumptions that suggest directions for future investigation. The collision model assumes perfect capture and does not account for successive interference cancellation. The idealized battery model does not capture capacity fade or temperature dependence. Multi-hop routing overhead and dynamic topology changes were not considered, nor were heterogeneous traffic patterns. Future work should extend this framework to incorporate these factors, conduct experimental validation on physical testbeds, and integrate it with real-world energy harvesting.

5. Conclusion

This study compared Always-On, SDC, and WuR-assisted communication strategies for battery-powered IoT networks over a 365-day simulation horizon. The results indicate that WuR provides a more effective architecture for long-term autonomous operation. WuR nodes maintained packet loss below 1.2% across network loads, whereas SDC reliability degraded superlinearly and reached approximately 16% packet loss under high-contention conditions. WuR also achieved an energy cost of 30.6 mJ per successful packet, corresponding to a 13.5-fold improvement over SDC, and supported a projected battery lifetime exceeding 1.5 years, compared with approximately 45 days for SDC. By decoupling energy efficiency from latency, WuR-assisted communication can support scalable and sustainable IoT networks. Future work should extend the framework to multi-hop routing, heterogeneous traffic, adaptive medium-access control, and experimental validation.

Declaration of generative ai

During the preparation of this manuscript, the authors used ChatGPT, version 4, for language editing and readability improvement. After using this tool, the authors carefully reviewed and edited the manuscript and take full responsibility for the final content.

Funding

This work was supported by Henan Provincial Key Science and Technology Research Project (Project No. 242102210182).

References

[1] A. Uzoka, E. Cadet, and P. U. Ojukwu, (2024) *"The role of telecommunications in enabling Internet of Things (IoT) connectivity and applications"* **Comprehensive Research and Reviews in Science and Technology** *2*: 55–73. DOI: 10.57219/crrst.2024.2.2.0037.

[2] S. L. Ullo and G. R. Sinha, (2020) *"Advances in smart environment monitoring systems using IoT and sensors"* **Sensors** *20*: 3113. DOI: 10.3390/s20113113.

[3] G. S. Kuaban, E. Gelenbe, T. Czachórski, P. Czekalski, and J. K. Tangka, (2023) *"Modelling of the energy depletion process and battery depletion attacks for battery-powered internet of things (iot) devices"* **Sensors** *23*: 6183. DOI: 10.3390/s23136183.

[4] J.-H. Park, Y.-J. Suh, D. Kim, H. Lee, H. Ahn, and Y. D. Park, (2025) *"MILD: Minimizing idle listening energy consumption via down-clocking for energy-efficient WI-fi communications"* **Sensors** *25*: 1155. DOI: 10.3390/s25041155.

[5] S. M. Vali, (2024) *"Enhancing coverage and efficiency in wireless sensor networks: A review of optimization techniques"* **Advances in Engineering and Intelligence Systems** ***3***: 39–52. DOI: 10.22034/aeis.2024.472891.1212.

[6] F. Amin, R. Abbasi, S. Khan, and M. A. Abid, (2022) *"An overview of medium access control and radio duty cycling protocols for internet of things"* **Electronics** ***11***: 3873. DOI: 10.3390/electronics11233873.

[7] B. Rana and Y. Singh. "Duty-cycling techniques in IoT: Energy-efficiency perspective". In: Springer, 2022, 505–512. DOI: 10.1007/978-981-16-8248-3_42.

[8] S. Chen, X. Yu, and X. Huang, (2025) *"Wake-up receivers: A review of architectures analysis, design techniques, theories and frontiers"* **Journal of Low Power Electronics and Applications** ***15***: 55. DOI: 10.3390/jlpea15040055.

[9] R. Sanchez-Vital, C. Gomez, and E. Garcia-Villegas, (2024) *"Exploring the boundaries of energy-efficient Wireless Mesh Networks with IEEE 802.11 ba"* **Internet of Things** ***28***: 101366. DOI: 10.1016/j.iot.2024.101366.

[10] S. L. Shah, Z. H. Abbas, G. Abbas, and N. H. Mahmood, (2025) *"Energy-efficient and reliable data collection in receiver-initiated wake-up radio enabled IoT networks"* **Computer Networks**: 111548. DOI: 10.1016/j.comnet.2025.111548.

[11] D. Liu, Z. Cao, H. Jiang, S. Zhou, Z. Xiao, and F. Zeng, (2022) *"Concurrent low-power listening: a new design paradigm for duty-cycling communication"* **ACM Transactions on Sensor Networks** ***19***: 1–24. DOI: 10.1145/3517013.

[12] M. A. Spohn, C. M. Ranieri, A. R. da Silva, and J. Ueyama, (2025) *"A systematic review on wake-up radios applied to wireless sensor networks"* **Journal of Computer Science** ***21***: 566–583. DOI: 10.3844/jcssp.2025.566.583.

[13] S. Wang, T. J. Odelberg, P. W. Crary, M. P. Obery, and D. D. Wentzloff, (2025) *"Low-power wake-up receivers for resilient cellular Internet of Things"* **Information** ***16***: 43. DOI: 10.3390/info16010043.

[14] L. Schulthess, S. Cortesi, and M. Magno. "WakeMod: A 6.9 µW Wake-Up Radio Module with–72.6 dBm Sensitivity for On-Demand IoT". In: *2025 10th International Workshop on Advances in Sensors and Interfaces (IWASI)*. IEEE, 2025, 1–6. DOI: 10.1109/IWASI66786.2025.11122000.

[15] R. Ding and W. Tatinian, (2025) *"Hierarchical scalable models of semi-active wake-up radio for wireless sensor network simulations"*: DOI: 10.36227/techrxiv.174495475.51279417/v1.

[16] S. M. S. Panga and S. S. Borkotoky. "Leveraging wake-up radios in UAV-Aided LoRa networks: Some preliminary results on a random-access scheme". In: *2023 17th International Conference on Telecommunications (ConTEL)*. IEEE, 2023, 1–7. DOI: 10.1109/ConTEL58387.2023.10199009.

[17] S. L. Shah, Z. H. Abbas, G. Abbas, F. Muhammad, A. Hussien, and T. Baker, (2023) *"An innovative clustering hierarchical protocol for data collection from remote wireless sensor networks based internet of things applications"* **Sensors 23**: 5728. DOI: 10.3390/s23125728.

[18] S. Mosavat, J. Göpfert, B.-C. Renner, P. J. Marrón, and M. Zella, (2025) *"Cato: Wake-up receiver-based communication for batteryless devices"* **Sensors 25**: 6813. DOI: 10.3390/s25226813.

[19] G. Leenders, G. Callebaut, G. Ottoy, L. V. der Perre, and L. D. Strycker, (2023) *"An energy-efficient LoRa multi-hop protocol through preamble sampling for remote sensing"* **Sensors 23**: 4994. DOI: 10.3390/s23114994.

[20] S. Hong, F. Yao, F. Zhang, Y. Ding, and S.-H. Yang, (2023) *"LPWC: Long preamble wake-up communication protocol for a LoRa network"* **Internet of Things 22**: 100787. DOI: 10.1016/j.iot.2023.100787.

[21] A. A. Deshpande, F. Chiariotti, and A. Zanella. "Energy-efficient internet of things monitoring with content-based wake-up radio". In: *2024 IEEE 35th International Symposium on Personal, Indoor and Mobile Radio Communications (PIMRC)*. IEEE, 2024, 1–6. DOI: 10.1109/PIMRC59610.2024.10817209.

[22] C. Rup and E. Bajic, (2024) *"Green and sustainable Industrial Internet of Things systems leveraging wake-up radio to enable on-demand IoT communication"* **Sustainability** ***16***: 1160. DOI: 10.3390/su16031160.

[23] M. Ghribi and A. Meddeb. "Performance evaluation of collision avoidance techniques using wake-up radio in WSNs". In: *2020 International Conference on Software, Telecommunications and Computer Networks (SoftCOM)*. IEEE, 2020, 1–6. DOI: 10.23919/SoftCOM50211.2020.9238258.

[24] Y. Luo and L. Pu, (2021) *"WUR-TS: Semi-passive wake-up radio receiver based time synchronization method for energy harvesting wireless networks"* **IEEE Transactions on Mobile Computing** ***21***: 4172–4186. DOI: 10.1109/TMC.2021.3064374.